

# CONVECTIVE SCALING OF THE AVERAGE DISSIPATION RATE OF TEMPERATURE VARIANCE IN THE ATMOSPHERIC SURFACE LAYER

GERARD KIELY,\* JOHN D. ALBERTSON, MARC B. PARLANGE\*\* and WILLIAM E. EICHINGER\*\*\*

*Hydrologic Science, University of California, Davis, CA 95616, U.S.A.*

(Received in final form 28 September, 1995)

**Abstract.** The flux of sensible heat from the land surface is related to the average rate of dissipation of temperature fluctuations in the atmospheric surface layer through the temperature variance budget equation. In many cases it is desirable to estimate the heat flux from measurement or inference of the dissipation rate. Here we study how the dissipation rate scales with atmospheric stability, using three inertial range methods to calculate the dissipation rate: power spectra, second order structure functions, and third order structure functions. Experimental data are analyzed from a pair of field experiments, during which turbulent fluctuations of velocity and temperature were measured over a broad range of neutral and unstable atmospheric flows. It is shown that the temperature dissipation rate scales with a single convective power law continuously from near-neutral to strongly unstable stratification. The dissipation scaling is found to nearly match production in the near-neutral region, but to be consistently lower than production in the more convective regimes. The convective scaling is shown to offer a simplified means of computing sensible heat flux from the dissipation rate of temperature variance.

## 1. Introduction

We study the average dissipation rate ( $\epsilon_\theta$ ) of temperature variance in the atmospheric surface layer (ASL) to investigate the range of stratification for which convective scaling is appropriate. We restrict our analysis to unstable and neutral thermal stratification in the ASL. This study is motivated by the contradictory scaling forms found for  $\epsilon_\theta$  in the literature and the belief that a convective scaling form for  $\epsilon_\theta$  will streamline greatly the estimation of heat fluxes from measured dissipation rates. The vertical flux of sensible heat is related to  $\epsilon_\theta$  through the temperature variance budget which, under stationary and horizontally homogenous conditions, is written

$$-\langle w\theta \rangle \frac{\partial \Theta}{\partial z} - \frac{1}{2} \frac{\partial \langle w\theta^2 \rangle}{\partial z} = \epsilon_\theta \quad (1)$$

where  $\Theta$  is the mean temperature,  $\theta$  the fluctuation about  $\Theta$ ,  $w$  represents the fluctuation in the vertical velocity, the vertical direction is  $z$  (upward from the land surface), and  $\langle \cdot \rangle$  is the averaging operator. The first term in (1) is the average rate

\* Permanent address: Department of Civil Engineering, University College, Cork, Ireland.

\*\* Also at Johns Hopkins University, Baltimore, Maryland.

\*\*\* Also at Los Alamos National Laboratory, Los Alamos, New Mexico.

of production of temperature variance by interaction of the vertical temperature flux  $\langle w\theta \rangle$  and the vertical mean temperature gradient. The second term represents the divergence of the turbulent flux of temperature variance. The third term is the average rate at which the temperature variance is dissipated, where  $\epsilon_\theta = D\langle (d\theta/dx_\alpha)(d\theta/dx_\alpha) \rangle$ , and  $D$  is the thermal diffusivity. Summation is implied on repeated subscripts. Note that (1) is written as a budget for  $1/2\langle \theta^2 \rangle$ , consistent with the turbulent kinetic energy (TKE) budget. The following scaling parameters will be applied to (1)

$$u_* = \sqrt{\frac{\tau_0}{\rho}} = \sqrt{-\langle uw \rangle}$$

$$\Theta_* = \frac{\langle w\theta \rangle}{u_*}$$
(2)

where  $u_*$  is the friction velocity,  $\tau_0$  the surface shear stress,  $\rho$  the average air density,  $u$  represents the fluctuation in the streamwise velocity component, and  $\Theta_*$  is the temperature scaling parameter. Substituting (2) into (1) we write the budget equation

$$-u_*\Theta_* \frac{\partial \Theta}{\partial z} - \frac{1}{2} \frac{\partial \langle w\theta^2 \rangle}{\partial z} = \epsilon_\theta.$$
(3)

From Monin–Obukhov similarity theory

$$\frac{\partial \Theta}{\partial z} = -\frac{\Theta_*}{kz} \Phi_H \left( \frac{z}{L} \right)$$

$$\epsilon_\theta = \frac{\Theta_*^2 u_*}{kz} \Phi_{\epsilon_\theta} \left( \frac{z}{L} \right)$$
(4)

where the similarity functions  $\Phi_H(z/L)$  and  $\Phi_{\epsilon_\theta}(z/L)$  are the normalized rates of production and dissipation,  $z/L$  is the dimensionless stability parameter, and the Obukhov length is defined as

$$L = \frac{-u_*^3 \Theta}{kg \langle w\theta \rangle}.$$
(5)

Substituting (4) into (3) and normalizing by  $u_* \Theta_*^2 / kz$  yields

$$\Phi_H \left( \frac{z}{L} \right) - \frac{kz}{u_* \Theta_*^2} \Lambda = \Phi_{\epsilon_\theta} \left( \frac{z}{L} \right)$$
(6)

where  $\Lambda$  represents the dimensional transport term. For context, we provide a brief review of the literature regarding the scaling of these dimensionless terms with surface-layer stratification, as represented by the stability parameter ( $z/L$ ).

The normalized production term has typically been expressed by the general Businger–Dyer interpolation formula

$$\Phi_H = \alpha_H \left( 1 - \beta_H \frac{z}{L} \right)^{-1/2} \quad (7)$$

where  $\alpha_H$  and  $\beta_H$  are empirical constants taken from experiments; typically,  $\alpha_H = 1$  and  $\beta_H = 16$  (Brutsaert, 1982). Högström (1988) provided a recent and detailed review of the scaling of  $\Phi_H$ . All, save one, of the forms for  $\Phi_H$  cited by Högström provide for scaling which asymptotes to  $(-z/L)^{-1/2}$  for large negative (convective) values of  $z/L$ . The one exception is Zilitinkevich and Chalikov (1968), where production is scaled as free convection  $(-z/L)^{-1/3}$  in the convective limit. The exponent in (7) is a much more fundamental parameter than the constants  $\alpha_H$  and  $\beta_H$  for it represents the asymptotic scaling of the temperature gradient (production) in the convective limit. Kader and Perepelkin (1984) described the convective scaling reasoning and proposed an abruptly discontinuous scaling form that captures the constant value of  $\Phi_H$  in the neutral limit and the  $-1/3$  scaling in the convective limit

$$\begin{aligned} \Phi_H &= 1.0 & \left( -\frac{z}{L} \right) &\leq 0.03 \\ \Phi_H &\propto \left( -\frac{z}{L} \right)^{-1/3} & \left( -\frac{z}{L} \right) &> 0.03. \end{aligned} \quad (8)$$

This idea of subdividing the ASL into layers has developed through the theoretical work of Betchov and Yaglom (1971) and studies by Kader (1988), Kader and Perepelkin (1989), and Kader and Yaglom (1990, hereafter KY), leading to the establishment of a three sublayer model of the ASL. KY provided extensive empirical support to the model and showed that the normalized production scales in the individual sublayers as

$$\begin{aligned} \Phi_H &= 0.96 & \left( -\frac{z}{L} \right) &\leq 0.04 \\ \Phi_H &= 0.33 \left( -\frac{z}{L} \right)^{-1/3} & 0.12 &< \left( -\frac{z}{L} \right) < 1.2 \\ \Phi_H &= 0.27 \left( -\frac{z}{L} \right)^{-1/3} & \left( -\frac{z}{L} \right) &> 2.0 \end{aligned} \quad (9)$$

where the constants have been modified to represent the inclusion of  $k$  ( $=0.4$ ), as KY made a point of omitting  $k$  from their analysis.

The dissipation term has received less direct study than the production term. Most authors that have addressed this term based their results on measurements made over narrow ranges of the stability parameter ( $z/L$ ) and presented the normalized dissipation as some percentage of measured production. In which case,

the exponent in the power law scaling of  $\Phi_H$  would be assumed to apply to  $\Phi_{\epsilon_\theta}$  as well. A review of the literature shows that the production : dissipation ratio in selective field studies varies over a range from 0.7 to 3.4 (e.g. Champagne *et al.*, 1977; Antonia *et al.*, 1979; Bradley *et al.*, 1981), with the mismatch attributed to the transport term. Wyngaard and Cote (1971) measured the transport term and concluded that it was an order of magnitude smaller than production, and that it varied from being a local sink at low values of  $-z/L$  to being a local source in the more convective cases. This is an important point, since the transport term must vary with height. In fact, as a divergence the transport term will not contribute to the global energy but rather will vanish when integrated over the full atmospheric boundary layer (ABL). For a more in depth review see Högström (1988; 1990). KY computed the average dissipation rate from power spectral scaling in the inertial subrange and reported the following fit to their three sublayer model

$$\begin{aligned} \Phi_{\epsilon_\theta} &= 0.84 & \left(-\frac{z}{L}\right) &\leq 0.04 \\ \Phi_{\epsilon_\theta} &= 0.25 \left(-\frac{z}{L}\right)^{-1/3} & 0.12 < \left(-\frac{z}{L}\right) < 1.2 \\ \Phi_{\epsilon_\theta} &= 0.19 \left(-\frac{z}{L}\right)^{-1/3} & \left(-\frac{z}{L}\right) > 2.0. \end{aligned} \quad (10)$$

From (9) and (10), we note that the implied production : dissipation ratio varies from 1.14 in the near-neutral region to 1.42 in the free convective region. This positive increase in the difference ( $\Phi_H - \Phi_{\epsilon_\theta}$ ) with height differs from the results of Wyngaard and Coté (1971) and it seems counter intuitive as we expect production to be greater near the wall with transport upward to support dissipation in the higher regions. Moreover, the decision to present separate model fits in the dynamic-convective and free-convective sublayers seems questionable for a variable such as  $\Phi_{\epsilon_\theta}$ , which is scaled by the same parameters in each of these two sublayers.

As alluded to above, knowledge of dissipation rates may be used to estimate the vertical fluxes between the Earth's surface and its atmosphere. This approach is used most often over the open ocean (Fairall and Larsen, 1986; deLeonibus and Simpson, 1987; Skupniewicz and Davidson, 1991; and Edson *et al.*, 1991), where more traditional methods such as eddy correlation become problematic due to ship motion. This approach is also useful for inferring heat fluxes from dissipation rates obtained from optical remote sensing instruments such as scintillometers (Andreas, 1988; Hill *et al.*, 1992) and lidar (Eichinger *et al.*, 1993). Regardless of the specific circumstances, all approaches to estimate fluxes from dissipation rates rest on the quality of the relationship between the dimensionless dissipation rate and the stability parameter ( $z/L$ ). And as we mentioned above, there exists a fundamental disagreement in the slope of this scaling for scalar dissipation rates. Therefore, we focus directly on our primary interest of the nondimensionalized dissipation rate and its scaling with  $z/L$ . The problem is addressed here through the acquisition of experimental data covering a wide range of neutral and unstable atmospheric

conditions and its analysis in the context of the three sublayer model. Note that in this paper, temperature  $\theta$  may be considered a proxy for other scalars (e.g. for specific humidity).

## 2. The Three Sublayer Model

The concept of the three sublayer model is discussed in detail by Kader and Yaglom (1990). For a short review see Albertson *et al.* (1995b). In brief, it subdivides the ASL into three regions (defined by ranges of  $z/L$ ) which are separated by narrow transition bands. At the bottom is the *Dynamic Sublayer* (DSL, where  $-z/L \leq 0.04$ ), just above which is the *Dynamic-Convective Sublayer* (DCSL, where  $0.12 \leq -z/L \leq 1.2$ ), and at the top is the *Free-Convective Sublayer* (FCSL, where  $-z/L \geq 2$ ). The DSL is dominated by mechanical shearing action such that buoyancy effects can be neglected, all velocity components are scaled with  $u_*$ , and temperature is scaled with  $\Theta_*$ . All one-point fluctuating moments are believed to be independent of  $z$  in the DSL, so the transport term in (6) vanishes (Kader and Yaglom, 1990). This implies that production equals dissipation

$$\Phi_{\epsilon_\theta} = \text{Const.} \sim \Phi_H \Rightarrow 1. \quad (11)$$

In the DCSL, the vertical velocity fluctuations scale with the convective velocity  $w_*$  ( $= [\langle w\theta \rangle g z / \Theta]^{1/3}$ ), and temperature is scaled with  $\Theta_{**}$  ( $= \langle w\theta \rangle / w_*$ ). For completeness we note that the horizontal velocity components scale with a longitudinal scaling velocity; but this is a moot point for the temperature variance budget equation as it includes strictly convective terms. Using these scaling parameters and conventional dimensional analysis on the budget equation gives

$$\Phi_{\epsilon_\theta} = \left( B_1 + \frac{1}{6} B_2 \right) \left( \frac{-z}{L} \right)^{-1/3} \quad (12)$$

where the constants  $B_1$  and  $B_2$  represent the respective contributions of production and transport. In the FCSL all velocity components scale with the convective velocity  $w_*$ , and the scaling temperature is  $\Theta_{**}$ . The dimensional analysis of the temperature variance budget is identical for the FCSL as for the DCSL, i.e. (Equation 12).

Recent experimental work (e.g. Kader and Yaglom, 1990) supports the dimensional analysis showing that both production  $\Phi_H$  and dissipation  $\Theta_{\epsilon_\theta}$  scale with  $(-z/L)^{-1/3}$  in these upper two sublayers.

## 3. Determination of $\epsilon_\theta$

The average rate of dissipation  $\epsilon_\theta$  of the variance of a turbulent temperature fluctuation may be computed using direct or indirect methods, in an analogous way to

that of velocity fluctuations (Tennekes and Lumley, 1972). However, direct methods require the measurement of the variance of the spatial or temporal derivatives of  $\theta$  with a resolution approaching the Kolmogorov microscale ( $\approx 1$  mm in the atmosphere). In this study a 3-D sonic anemometer with a transponder spacing of 150 mm is used to support analysis using indirect methods based on inertial subrange scaling of: (i) spectral densities, (ii) second-order structure functions, and (iii) third-order structure functions. Taylor's (1938) hypothesis of frozen turbulence is used to convert time series at a point to "spatial series" along the line of flow, as needed for the inertial subrange scaling.

1) *Spectral Density*: In the Kolmogorov inertial subrange, the spectral density of the temperature signal is described as (Corrsin, 1951)

$$E_{\theta}(k) = \beta_{\theta} \epsilon_{\theta} \epsilon^{-1/3} k^{-5/3} \quad (13)$$

where  $E_{\theta}$  is the expected power of the turbulent temperature fluctuations at wavenumber  $k$  ( $\text{rad m}^{-1}$ ), and  $\beta_{\theta}$  is the Obukhov–Corrsin constant, which is taken as 0.8 in this study, following Wyngaard and Cote (1971), Bradley *et al.* (1981), and Kaimal and Finnigan (1994). To solve for  $\epsilon_{\theta}$  using (13), we use the average rate of dissipation ( $\epsilon$ ) of TKE obtained from a regression of the spectral density of the longitudinal velocity fluctuations

$$E_u(k) = \alpha_u \epsilon^{2/3} k^{-5/3} \quad (14)$$

where  $\alpha_u$  is the Kolmogorov constant, taken as 0.55 (e.g. Antonia *et al.*, 1979; Kaimal and Finnigan, 1994).

2) *Second-Order Structure Function*: The second-order structure function represents the expected value of the temperature difference between two points separated by a distance  $r$  along the flow direction as a function of that distance  $r$ , viz. ( $D_{\theta\theta}(r) = \langle (\Delta\theta(r))^2 \rangle$ ) where we write  $\Delta\theta(r)$  for  $\theta(x+r) - \theta(x)$  (Monin and Yaglom, 1975). The second-order structure function for temperature is related to the dissipation rate in the inertial subrange as (Obukhov, 1949)

$$D_{\theta\theta}(r) = C_{\theta\theta} \epsilon_{\theta} \epsilon^{-1/3} r^{2/3} \quad (15)$$

where under a constant skewness assumption the constant  $C_{\theta\theta} = 4.0\beta_{\theta}$ . For the structure function approach we obtain  $\epsilon$  from a regression of the second-order structure function for longitudinal velocity fluctuations, which scales according to Kolmogorov's (1941) second hypothesis as

$$D_{uu}(r) = C_{uu} \epsilon^{2/3} r^{2/3} \quad (16)$$

where the constant skewness assumption gives  $C_{uu} = 4.0\alpha_u$ .

3) *Third-Order Structure Function*: The mixed third-order structure function represents the expected value of the product of the longitudinal velocity difference and the squared temperature difference as a function of  $r$ , where  $r$  is the distance along the flow direction over which the differences are taken, viz

$$D_{u\theta\theta}(r) = \langle (u(x+r) - u(x))(\theta(x+r) - \theta(x))^2 \rangle. \quad (17)$$

The mixed third order structure function (Yaglom, 1949; Monin and Yaglom, 1975, p. 495) scales in the inertial subrange as

$$D_{u\theta\theta}(r) = -\frac{4}{3}\epsilon_{\theta}r. \quad (18)$$

This latter method is particularly attractive since there are no free constants, and (18) does not depend on *a priori* knowledge of the dissipation rate of the turbulent kinetic energy, as required by the spectral and second-order structure function methods.

#### 4. Experiment

Two experiments were performed to investigate the effect of atmospheric stability on the normalized dissipation rate of temperature variance. Each experiment involved measurements of the surface energy balance and atmospheric turbulence. The first experiment was at the Campbell Tract research facility at the University of California at Davis, and the second was at the dry Owens Lake, at the southern end of the Owens Valley in southeastern California. In each case a one-dimensional sonic anemometer with a fine wire (diameter 0.0127 mm) thermocouple and a Krypton hygrometer were used (at 10 Hz with covariances taken over 20 minute periods) to measure the vertical fluxes of sensible and latent heat. A 3-D sonic anemometer (Gill Instruments 1012R2) was used to log the three velocity components and the speed of sound. The 3-D sonic was operated at 21 Hz during the Davis experiment and 56 Hz at Owens Lake.

The Davis site consists of a uniform bare soil field, extending 500 m by 500 m. In the northeast corner of the field there is an irrigated portion extending 155 m in the north-south direction and 115 m in the east-west direction. The surface roughness length has been estimated at  $z_0 = 2$  mm. The prevailing winds are from the southwest. The fetch exceeds 100 m for uniform surface wetness, and 400 m for uniform surface roughness. The 3-D sonic was positioned at  $z = 0.85$  m on June 22, 23, 24 and 25, 1994 and at  $z = 1.5$  m on July 15, 1994. Irrigation of the site was performed over the nights of June 21 and July 14 with periods of drying in between. By saturating the soil surface we forced most of the available energy to latent heat rather than sensible heat, thus extending the range of near-neutral flows in the DSL available for experimental investigation. A wide range of atmospheric

stability conditions were encountered, with the days following immediately after irrigation having low  $-z/L$  values and  $-z/L$  increasing with time following irrigation, as more energy is partitioned to sensible heat flux and so increasing buoyant production.

To encounter a broader range of convective conditions, measurements were made over the extremely arid dry Owens Lake. The Owens Lake site is part of a large basin situated between the Sierra Nevada to its west and the White and Inyo Mountains to its east. The surface is a crusted sand with a large fraction of evaporative salts. The surface area of the lakebed exceeds  $200 \text{ km}^2$ , and the uniform fetch at the experimental site exceeds 10 km. The surface roughness length ( $z_0$ ) is approximately 0.13 mm (Katul *et al.*, 1995). Surface energy balance measurements and 56 Hz atmospheric turbulence measurements were made at  $z = 2.65 \text{ m}$  during the experimental period from August 8 to 12, 1994.

Temperature was obtained from speed of sound measurements obtained from the 3-D sonic anemometer. The fluctuations in the speed of sound are due to fluctuations in the air density, which is attributed to fluctuations in water vapor concentration and air temperature. The speed of sound (density) fluctuations are measured directly by the 3-D sonic, thus providing fast response temperature fluctuation data from (Feynman *et al.*, 1963, p. 47–7; Kaimal and Finnigan 1994, p. 216)

$$c^2 = 403(\Theta + \theta) \left( 1 + 0.32 \frac{e}{p} \right) \quad (19)$$

where  $c$  is the speed of sound,  $(\Theta + \theta)$  is the instantaneous absolute temperature,  $e$  is the water vapor pressure and  $p$  is the atmospheric pressure. The effect of water vapor fluctuations on (19) were neglected for the arid Owens Lake site. The temperature derived from (19) has been compared favorable to that from a fine wire thermocouple and has been applied successfully in other studies (Katul *et al.*, 1995; Albertson *et al.*, 1995a).

## 5. Results

Of the data collected, 180 files (20 minutes each) were selected for analysis on the basis of having turbulence intensity ( $TI = \sigma_u / \langle U \rangle$ ) values less than 50% (for the reliable application of Taylor's (1938) hypothesis, values of  $TI \lesssim 30\%$  are usual – see Lumley and Panofsky (1964) – but we have included files with higher values since our analysis shows normalized dissipation values to be insensitive to  $TI$  for  $TI$  values less than 50%). The Davis experiment provided 105 of these files, and the remaining 75 are from the Owens Lake site. Figure 1a, 1b and 1c are typical plots of the spectra, second-order structure functions and mixed third-order structure functions, respectively. They follow generally their requisite scaling slopes of  $-5/3$ ,  $2/3$ , and 1. Of the three methods used, the third-order structure function is



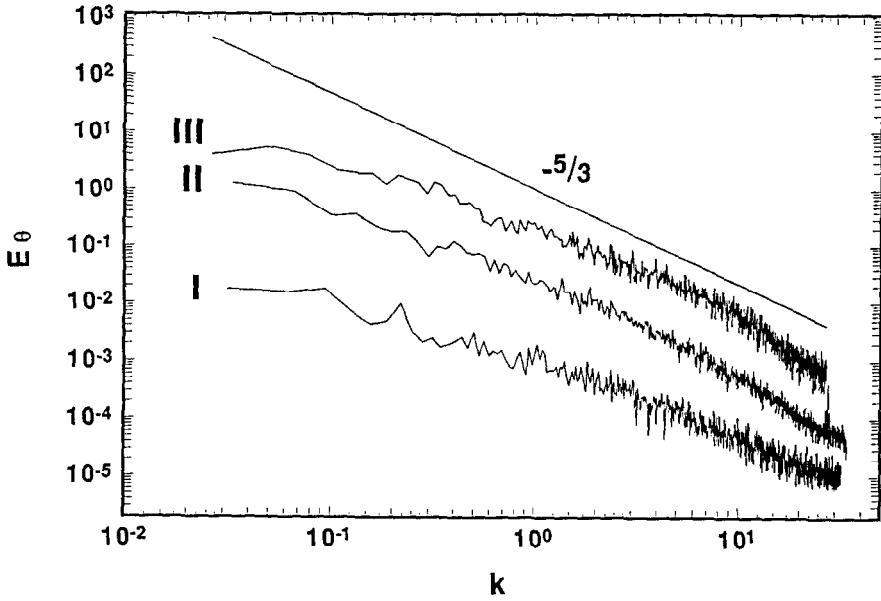


Figure 1a. Power spectra of temperature fluctuations ( $\theta$ ) for three sample sata files ( $k$  is wavenumber [rad/m]). I represents DSL, II DCSL, and III FCSL. The spectra have been shifted apart for presentation, so the absolute magnitudes of  $E_\theta$  should be disregarded.

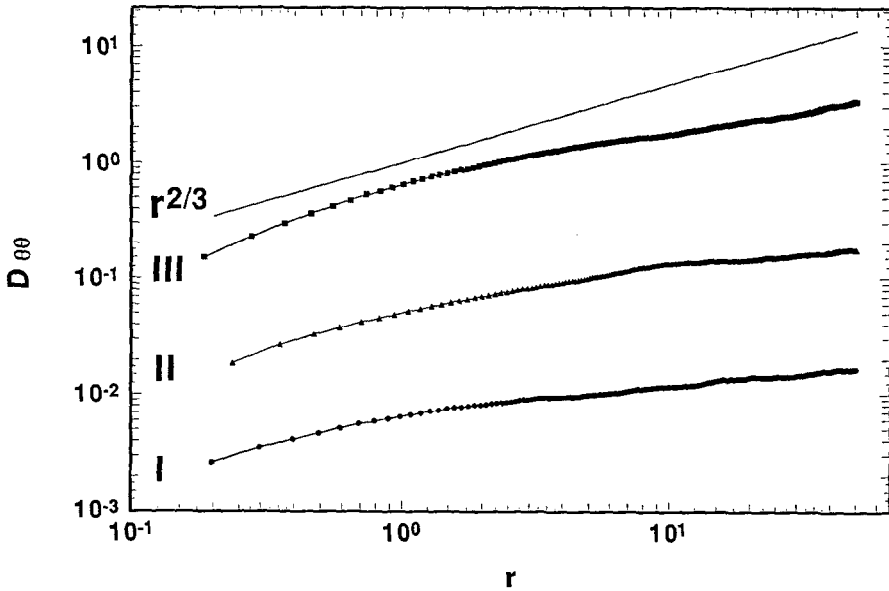


Figure 1b. Second order structure functions for the same three sample files shown in Figure 1a ( $r$  is lag [m]). The plots have been shifted for presentation.

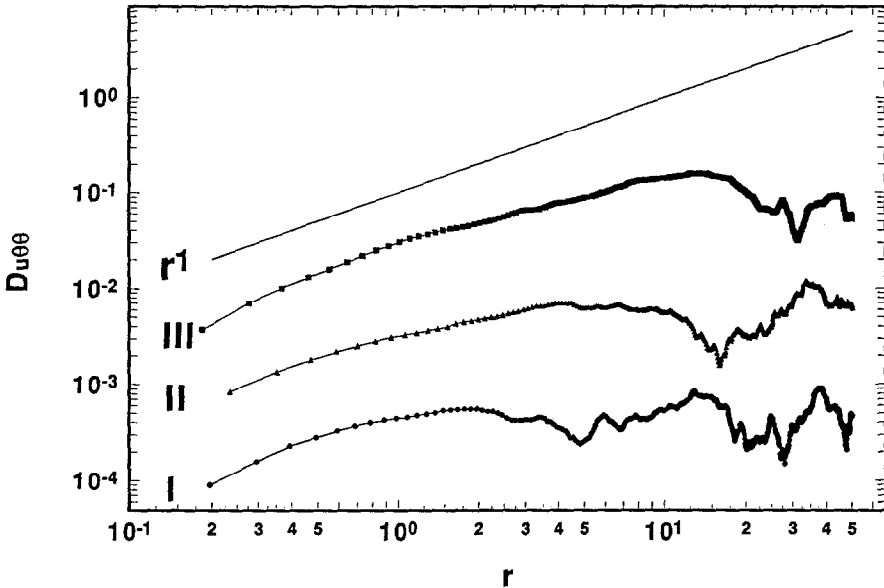


Figure 1c. Third order structure functions for the same three sample files shown in Figure 1a ( $r$  is lag [m]). The plots have been shifted for presentation.

considered to be a more stringent test of inertial subrange scaling. It was, therefore, used in this study to delineate the inertial subrange.

Figures 2a, 2b and 2c show the normalized dissipation rates  $\Phi_{\epsilon_\theta}$  as computed from regressions of (13)–(18) for the spectra, second-order structure functions, and third-order structure functions, respectively. Regressions were performed within the inertial subrange, as identified by the behaviour of the third-order structure function and constrained to represent lags not smaller than the transponder spacing and not larger than one-half the height of the instrument. The solid line represents production  $\Phi_H$  as computed by (7) with  $\alpha_H = 1$  and  $\beta_H = 16$ . The normalized dissipation rates fall below this line in the DCSL and FCSL regions. In the DSL, the production line tends towards the horizontal to a value of slightly less than 1. The  $\Phi_{\epsilon_\theta}$  data are close to unity in this region also, with the exception of one noted outlier – which happens to represent the most neutral run in the experiment.

Figure 3 represents the data as averaged in bins of equal  $\log(-z/L)$  spacing. The spectral method yields higher values of  $\Phi_{\epsilon_\theta}$  than the values of  $\Phi_{\epsilon_\theta}$  from the second-order structure function, which, in turn, are slightly higher than  $\Phi_{\epsilon_\theta}$  values from the mixed third-order structure function. The values of  $\Phi_{\epsilon_\theta}$  computed from the spectral and second-order structure function methods must be considered in the context of the uncertainty associated with the values of the constants (i.e.  $\alpha_u$ ,  $\beta_\theta$ ,  $C_{uu}$ ,  $C_{\theta\theta}$ ) used in the inertial subrange regression. Typical values of  $\alpha_u$  range from 0.5 to 0.62 and  $\beta_\theta$  from 0.7 to 1.0 (e.g. Antonia *et al.*, 1979). To show the effect of these constants on the  $\Phi_{\epsilon_\theta}$  values, we present limits (or bounds) in Figure 3, with

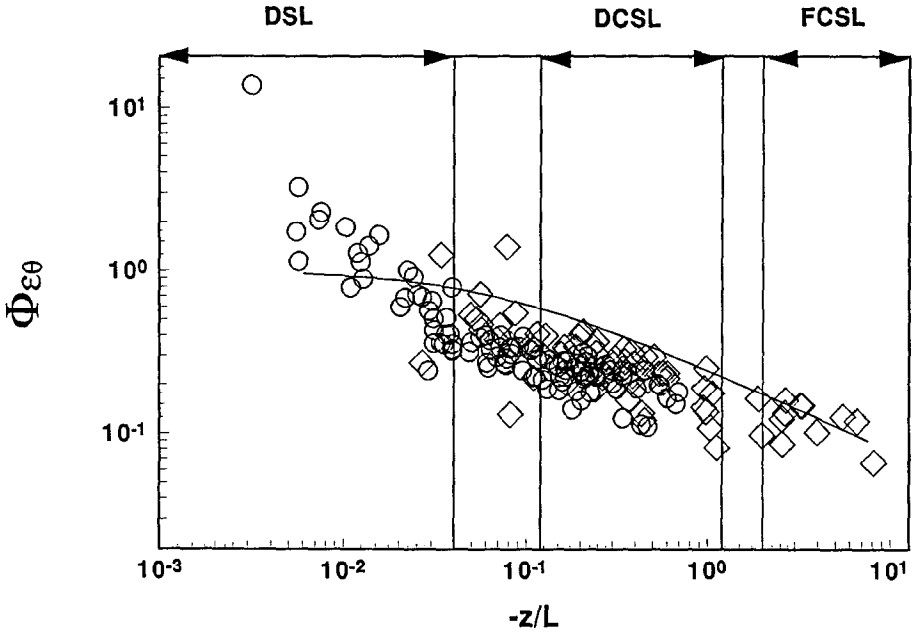


Figure 2a. Power spectra based estimates of the normalized dissipation rates versus atmospheric stability for the 180 files. The Campbell Tract points are marked by circles, and the Owens Lake points with diamonds. The estimated normalized rate of production  $\Phi_H$  of temperature variance (based on Businger-Dyer formula with  $\alpha_H = 1$  and  $\beta_H = 16$ ) is shown with a solid line.

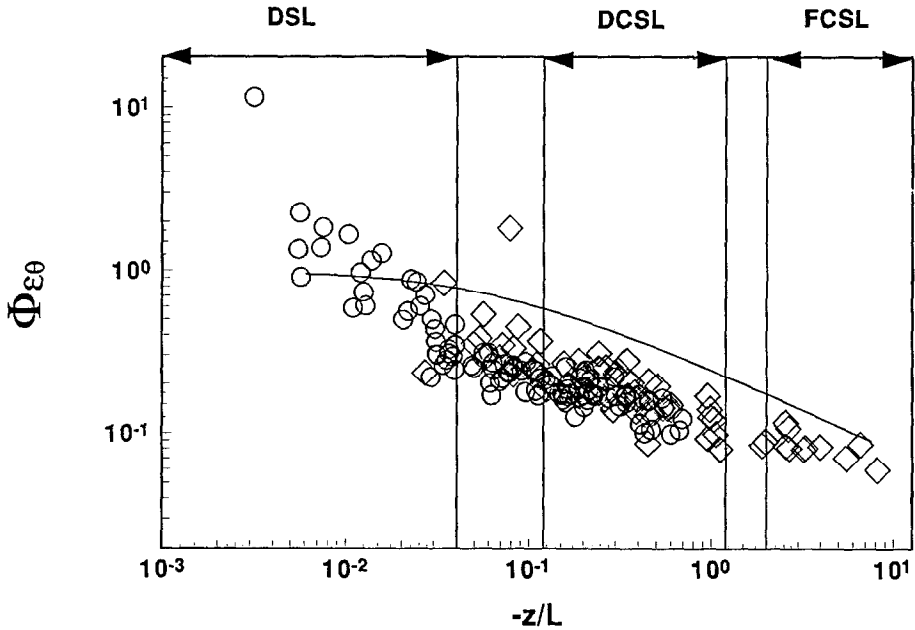


Figure 2b. Second-order structure function based estimates of the normalized dissipation rates versus atmospheric stability for the 180 files. Production line and symbols are as in Figure 2a.

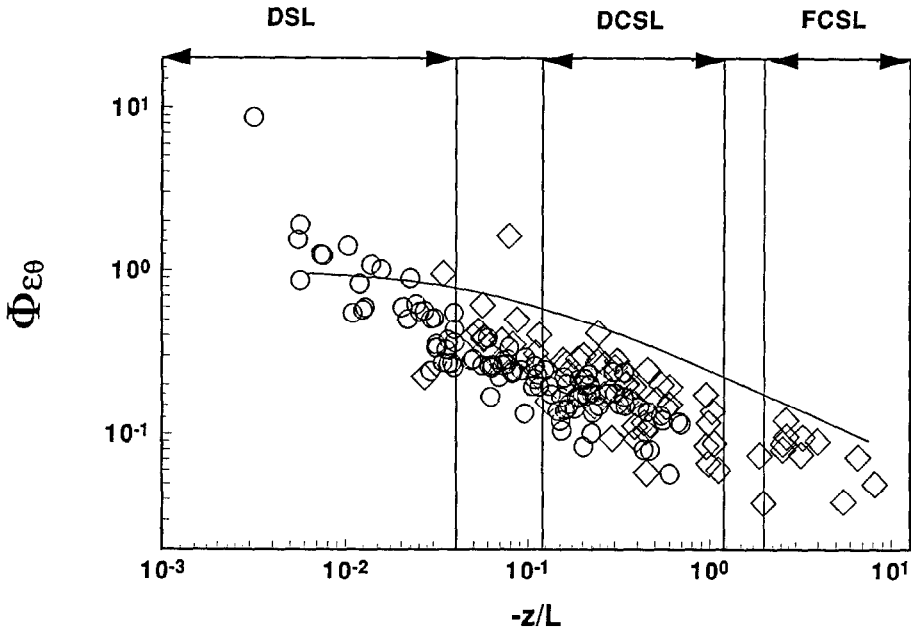


Figure 2c. Third-order structure function based estimates of the normalized dissipation rates versus atmospheric stability for the 180 files. Production line and symbols are as in figure 2a.

the upper limit based on using  $\alpha_u = 0.5$  and  $\beta_\theta = 0.7$  for the spectral based values and the lower limit based on using  $C_{uu} = 2.5$  (i.e.  $\alpha_u = 0.62$ ) and  $C_{\theta\theta} = 4.0$  (i.e.  $\beta_\theta = 1.0$ ) for the second-order structure function based values. The third-order structure function approach does not contain a free constant, and the results based on this method fall within the presented bounds. Considering the uncertainty introduced to the second-order methods by the inertial range scaling constants, we place more confidence in the results from the mixed third-order structure function, and, therefore, base our conclusions on these.

In Figure 4, we analyze further the results of the third-order structure function method. The three sublayer model was least-squares fitted to the unbinned data of Figure 2c. In the DSL, the fit was to (11). To investigate the appropriateness of separate scaling equations in the two convective sublayers, we regressed separate fits to (12) in each the DCSL and the FCSL, as was done by Kader and Yaglom (1990). However, the regressions yielded the same values for the constants in the DCSL and the FCSL. The resulting scaling is

$$\begin{aligned}
 \Phi_{\epsilon\theta} &= 0.88 && \left( \frac{-z}{L} < 0.04 \right) \\
 \Phi_{\epsilon\theta} &= 0.11 \left( \frac{-z}{L} \right)^{-1/3} && \left( 0.12 < \frac{-z}{L} \right)
 \end{aligned}
 \tag{20}$$

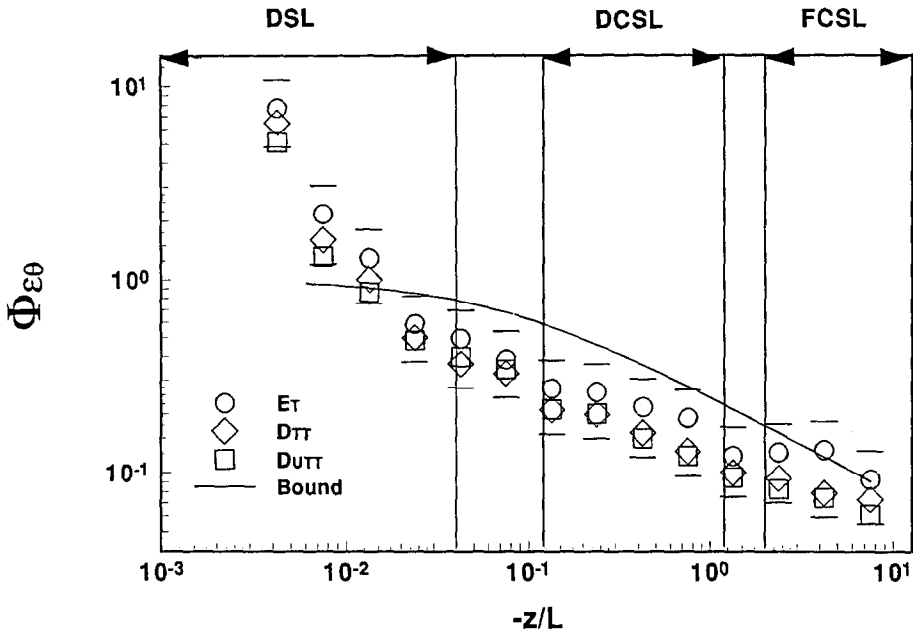


Figure 3. Data from Figures 2a, 2b, and 2c, placed in logarithmically spaced bins. Average of data in each bin showed with circles for the spectral estimates, diamonds for the second-order structure functions estimates, and squares for the third-order structure function estimates. Bounds are shown to represent the effect of using a range of inertial range constants. The normalized production line is shown as on Figures 2.

which is shown on Figure 4. If we adjust the results (10) of Kader and Yaglom (1990) to reflect a change of  $\beta_\theta$  from the 0.7 value used in their analysis to the 0.8 value selected in the present paper, we find their three constants to be 0.70, 0.21, and 0.16 in the DSL, DCSL, and FCSL, respectively. We note from Figure 4 that it may be desirable in practice to represent the full unstable and near-neutral range by a single convectively scaled model for normalized dissipation. To explore this, (12) was least squares fitted to the full range of data ( $0.006 < -z/L < 8$ ) in Figure 2c, yielding a single convective power law relationship for all negative values of  $z/L$

$$\Phi_{\epsilon_\theta} = 0.12 \left( \frac{-z}{L} \right)^{-1/3} \tag{21}$$

(note: the most neutral point was omitted from the regression as an outlier).

This simple scaling form (21) submits to closed form solution for sensible heat fluxes with measurements of  $\epsilon_\theta$ . By substituting (2), the definition of  $\Phi_{\epsilon_\theta}$  from (4), and (5) into (21) we write the sensible heat flux  $H (= \rho c_p \langle w\theta \rangle)$  as

$$H = (0.12)^{-3/5} \rho c_p \left( \frac{g}{\Theta} \right)^{1/5} (kz)^{4/5} \epsilon_\theta^{3/5} \tag{22}$$

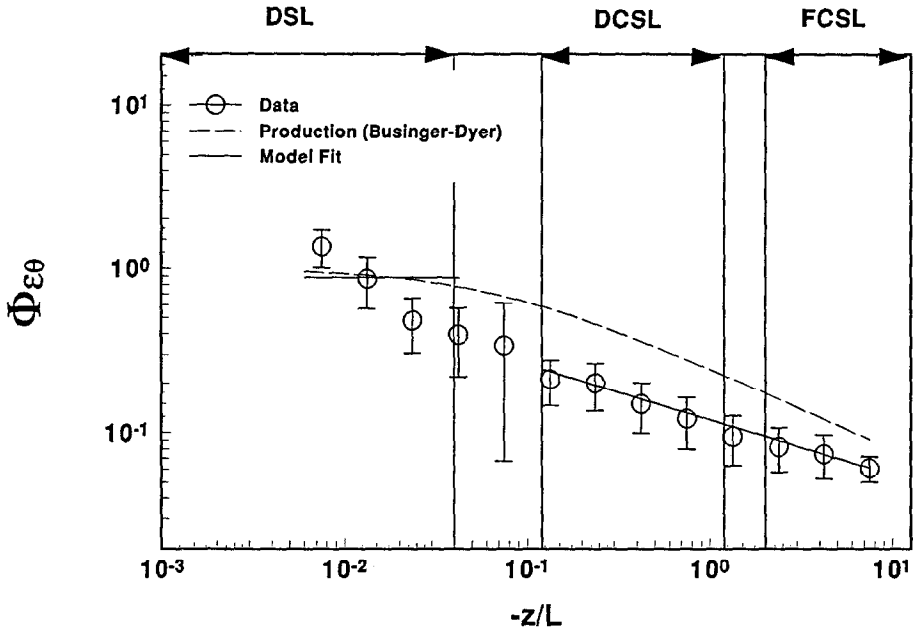


Figure 4. Data from Figure 2c placed in logarithmically spaced bins. The average of the  $\Phi_{\epsilon_\theta}$  data in each bin is represented with an open circle, and the standard deviations are marked with vertical bars. The Businger-Dyer production model is shown as a dashed line and the derived dissipation scaling (20) is plotted with the solid line. The near-neutral outlier of figure 2c has been omitted.

where  $\epsilon_\theta$  may be taken from inertial subrange scaling of measurements of  $u$  and  $\theta$ . To examine the performance of (22), it was used to estimate  $H$  with the measurements of  $\epsilon_\theta$  from the third-order structure function regressions. These estimates of  $H$  are compared to the eddy correlation based measurements of  $H$  in Figure 5. Note that the comparison is for the same files used to calculate the coefficient in (21). Future studies are planned to evaluate the performance of (22) with independent data. The evaluation here is simply for demonstration purposes.

## 6. Discussion

Dimensional analysis when applied to the three sublayer model of the ASL suggests a constant value for the normalized dissipation rate of temperature variance ( $\Phi_{\epsilon_\theta}$ ) in the dynamic sublayer, and a simple scaling with  $(-z/L)^{-1/3}$  in the increasingly unstable dynamic-convective and free-convective sublayers. This result has been compared to experimentally derived values of  $\Phi_{\epsilon_\theta}$ , where the UC Davis Campbell Tract experiment provided near-neutral flows under irrigated conditions and the dry Owens lakebed experiment provided highly unstable atmospheric stratification.

All three of the methods used to measure indirectly the average dissipation rate confirm the predicted scaling, with a potential discrepancy in the DSL, which may

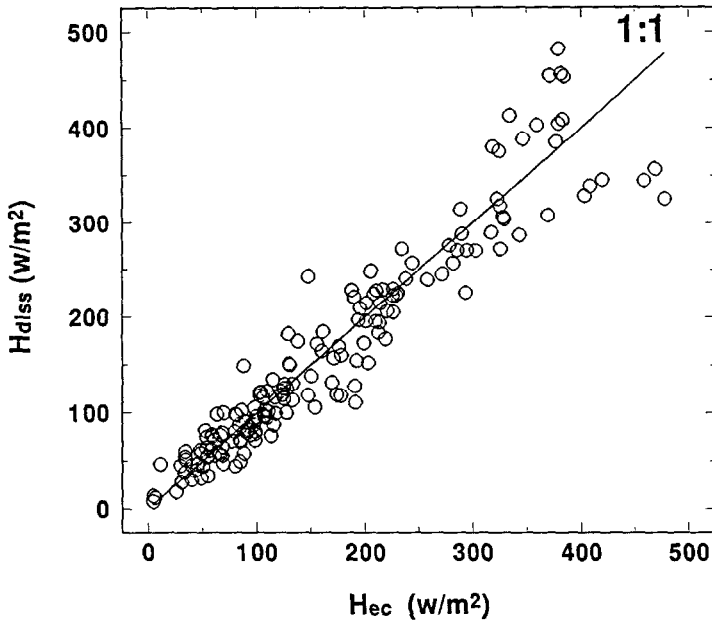


Figure 5. Comparison of sensible heat flux estimates from the revised inertial-dissipation model ( $H_{diss}$ ) with direct measurements from eddy correlation ( $H_{ec}$ ). A 1:1 line is shown for aid in comparison.  $H_{diss}$  regressed against  $H_{ec}$  yields  $R^2 = 0.91$  and a slope of 0.97.

be attributed to either spurious over-prediction of  $\Phi_{\epsilon_\theta}$  at very low  $-z/L$  or true convective scaling (i.e.  $-1/3$  power) of  $\Phi_{\epsilon_\theta}$  for flows in the DSL. Most likely the high values in the DSL are due to hyper-sensitivity of the normalizing process as  $\Theta_*$  in the denominator heads toward 0 in the neutral limit. However, it may be desirable in practice to represent the full unstable and near-neutral range by a single convectively scaled model for normalized dissipation.

The dissipation rates are found to match production rates in the DSL and to be systematically lower than production in the DCSL and FCSL, with an equality approached under the most convective conditions. Our results do not directly support Monji's (1973) claim that the transport term changes sign at  $-z/L = 1$ . However, we do see the gap between production and dissipation narrowing as  $-z/L$  increases. Monji suggested that as  $z$  becomes  $> |L|$ , the transport becomes a local source. This does make qualitative sense, as a mechanism other than production is required to maintain temperature fluctuations in the higher regions where production is vanishing. We may conclude that dissipation is lower than production in the lower ASL as the produced variance is being transferred up to higher levels within say the mixed layer, where production of temperature variance is effectively absent and dissipation is still present.

The third order mixed structure function has been found to be a simple method of operationally obtaining  $\epsilon_\theta$ , without requiring the intermediate calculation of  $\epsilon$  as required by the two second-order approaches. Another attribute of the third-order

approach is the fixed nature of its inertial subrange constant. The  $\Phi_{\epsilon\theta}$  results from this method have been shown to fall within the potential limits of estimates from second-order approaches, when the Kolmogorov constants are allowed to vary over a narrow, acceptable range.

The model fitting to the third-order derived  $\Phi_{\epsilon\theta}$  values in the three sublayers (20) resulted in identical coefficients for the DCSL and FCSL. This suggests that the division of the convective region into two separate sublayers (DCSL and FCSL) may be meritless when addressing variable groups such as  $\Phi_{\epsilon\theta}$ , in which all terms scale convectively throughout the region covered by the two sublayers.

The convective scaling form was shown to provide a simple and direct means of estimating surface heat flux from third-order structure function analysis of  $u$  and  $\theta$  measurements. Similar results could be expected for other scalars such as humidity. This revised inertial-dissipation method of computing heat fluxes avoids many of the problems of the previous approach, such as: the effects of uncertain inertial subrange constants; the need to explicitly calculate  $\epsilon$  before  $\epsilon\theta$ ; the effect of extensive data manipulation (e.g. windowing, tapering, averaging) in the power spectral scaling; and, the iterative solution scheme.

### Acknowledgements

The authors wish to thank Anthony Cahill and Mike Mata for their assistance in the field, and Scott Tyler for his support and assistance during the Owens Lake experiment. This research has been supported and financed, in part, by the Great Basin Pollution Control District, the National Science Foundation (EAR-93-04331), CA State Salinity Drainage Task Force, Kearney Foundation, CA Water Resources Center (W-182), the UC Davis Superfund grant (5P42ES04699-07), and the NASA Graduate Student Fellowship in Global Change Research program.

### References

- Albertson, J. D., Parlange, M. B., Katul, G. G., Chu, C.-R., Stricker, H. and Tyler, S.: 1995a, 'Sensible Heat Flux from Arid Regions: A Simple Flux-Variance Method', *Water Resour. Res.* **31**, 969–973.
- Albertson, J. D., Kiely, G., Parlange, M. B. and Eichinger, W. E.: 1995b, 'The Average Dissipation Rate of Turbulent Kinetic Energy in the Neutral and Unstable Atmospheric Surface Layer', *J. Geophys. Res.* submitted.
- Andreas E. L.: 1998, 'Using Scintillation at Two Wavelengths to Measure Path-Averaged Heat Fluxes in Free Convection', *Boundary-Layer Meteorol.* **54**, 167–182.
- Antonia, R. A., Chambers, A. J., Phong-Anant, D. and Rajagopalan, S.: 1979, 'Properties of Spatial Temperature Derivatives in the Atmospheric Surface Layer', *Boundary-Layer Meteorol.* **17**, 101–118.
- Betchov, R. and Yaglom, A. M.: 1971, 'Comments on the Theory of Similarity as Applied to Turbulence in an Unstably Stratified Fluid', *Izv., Atmos. Ocean. Phys.* **7**, 1270–1279, (829–834 in English translation).
- Bradley, E. F., Antonia, R. A. and Chambers, A. J.: 1981, 'Temperature Structure in the Atmospheric Surface Layer', *Boundary-Layer Meteorol.* **20**, 275–292.



- Brutsaert, W.: 1982, *Evaporation Into the Atmosphere*, 299 pp., Kluwer Academic Publishers.
- Brutsaert, W.: 1992, 'Stability Correction Functions for the Mean Wind Speed and Temperature in the Unstable Surface Layer', *Geophys. Res. Letters*, **19**, 469–472.
- Champagne, F. H., Friehe, C. A., LaRue, J. C. and Wyngaard, J. C.: 1977, 'Flux Measurements, Flux Estimation Techniques, and Fine-Scale Turbulence Measurements in the Unstable Surface Layer over Land', *J. Atmos. Sci.* **34**, 515–530.
- Corrsin, S.: 1951, 'On the Spectrum of Isotropic Temperature Fluctuations in an Isotropic Turbulence', *J. Appl. Phys.* **22**, 469–473.
- DeLeonibus, P. S. and Simpson, L. S.: 1987, 'Dissipation Observations of Drag Coefficients Over the Open Ocean', *IEEE J. Oceanic Eng.* **OE-12**, 296–300.
- Edson, J. B., Fairall, C. W., Mestayer, P. G. and Larssen, S. E.: 1991, 'A Study of the Inertial-Dissipation Method for Computing Air-Sea Fluxes', *J. Geophys. Res.* **96C**, 10689–10711.
- Eichinger, W. E., Cooper, D. I., Holtkamp, D. B., Karl Jr., R. R., Quick, C. R. and Till, J. J.: 1993, 'Derivation of Water Vapour Fluxes from Lidar Measurements', *Boundary-Layer Meteorol.* **63**, 39–64.
- Fairall, C. W., Edson, J. B., Larsen, S. E. and Mestayer, P. G.: 1990, 'Inertial-dissipation Air-Sea Measurements: a Prototype System Using Realtime Spectral Computations', *J. Atmos. Ocean. Tech.* **7**, 425–453.
- Fairall, C. W. and Larsen, S. E.: 1986, 'Inertial-Dissipation Methods and Turbulent Fluxes at the Air-Ocean Interface', *Boundary-Layer Meteorol.* **34**, 287–301.
- Feynman, R. P., Leighton, R. B. and Sands, M.: 1963, *The Feynman Lectures on Physics*, Vol. 1, Addison-Wesley.
- Hill, R. G., Ochs, G. R. and Wilson, J. J.: 1992, 'Measuring Surface Layer Fluxes of Heat and Momentum Using Optical Scintillation', *Boundary-Layer Meteorol.* **58**, 391–408.
- Högström, U.: 1988, 'Non-Dimensional Wind and Temperature Profiles', *Boundary-Layer Meteorol.* **42**, 55–78.
- Högström, U.: 1990, 'Analysis of Turbulence Structure in the Surface Layer with a Modified Similarity Formulation for near Neutral Conditions', *J. Atmos. Sci.* **47**, 1949–1972.
- Kader, B. A.: 1988, 'Three-Level Structure of an Unstably Stratified Atmospheric Surface Layer', *Izv. Atmos. Ocean. Phys.* **24**, 907–919 (English translation).
- Kader, B. A.: 1992, 'Determination of Turbulent Momentum and Heat Fluxes by Spectral Methods', *Boundary-Layer Meteorol.* **61**, 323–347.
- Kader, B. A. and Perepelkin, V. G.: 1984, 'Profiles of the Wind Velocity and Temperature in the Near-Surface Layer of the Atmosphere under Conditions of Neutral and Unstable Stratification', *Izv. Atmos. Ocean. Phys.* **20**, 112–119, (English translation).
- Kader, B. A. and Perepelkin, V. G.: 1989, 'Effect of Unstable Stratification on the Wind Speed and Temperature Profiles in the Surface Layer', *Izv. Atmos. Ocean. Phys.* **25**, 583–588, (English translation).
- Kader, B. A. and Yaglom, A. M.: 1990, 'Mean Fields and Fluctuation Moments in Unstably Stratified turbulent Boundary Layers', *J. Fluid Mech.* **212**, 637–662.
- Kaimal, J. C. and Finnigan, J. J.: 1994, *Atmospheric Boundary Layer Flows. Their Structure and Measurement*, Oxford University Press, 289p.
- Katul, G. G., Chu, C.-R., Parlange, M. B., Albertson, J. D. and Ortenburger, T. A.: 1995, 'Low-Wavenumber Spectral Characteristics of Velocity and Temperature in the Atmospheric Surface Layer Flows', *J. Geophys. Res.* **100**, 1424–14255.
- Kolmogorov, A. N.: 1941, 'The Local Structure of Turbulence in Incompressible Viscous Fluid for very Large Reynolds Number', *Dokl. Akad. Nauk. SSSR*, **30**, 301–303.
- Lumley, J. L. and Panofsky, H. A.: 1964, *The Structure of Atmospheric Turbulence*, Wiley Interscience, New York, 239 pp.
- Monin, A. A. and Yaglom, A. M.: 1975, *Statistical Fluid Mechanics*. Vol. II, J. Lumley (ed.), MIT Press, 874 pp.
- Monji, N.: 1973, 'Budgets of Turbulent Energy and Temperature Variance in the Transition Zone from Forced to Free Convection', *J. Meteorol. Soc. Japan* **51**, 133–145.
- Obukhov, A. M.: 1949, 'Structure of the Temperature Field in a Turbulent Flow', *Izv. Akad. Nauk. SSSR, Ser. Geogr. i. Grafiz.* **13**, 58–69.

- Skupniewicz, C. E. and Davidson, K. L.: 1991, 'Hot-Film Measurements from a Small Buoy: Surface Wind Estimates Using the Inertial Dissipation Method', *J. Atmos. Ocean. Tech.* **8**, 309–322.
- Taylor, G. I.: 1938, 'The Spectrum of Turbulence', *Proc. Roy. Soc., A*, **CLXIV**, 476–490.
- Tennekes, H. and Lumley, J.: 1972, *A First Course in Turbulence*, MIT Press, 300 pp.
- Wyngaard, J. C. and Cotè, O. R.: 1971, 'The Budgets of Turbulent Kinetic Energy and Temperature Variance in the Atmospheric Surface Layer', *J. Atmos. Sci.* **28**, 190–201.
- Yaglom, A. M.: 1949, 'Homogeneous and Isotropic Turbulence in a Viscous Compressible Fluid', *Izv. Akad. Nauk SSSR Ser. Geogr. i Geofiz.* **12**, 501–522.
- Zilitinkevich, S. S. and Chalikov, D. V.: 1968, 'Determining the Universal Wind-Velocity and Temperature Profiles in the Atmospheric Boundary Layer', *Izv. Atmos. Ocean. Phys.* **4**, 294–302 (English Translation, pp. 165–170).